Mathematical Morphology Applied to the Study of Dual Phase Steel Formation

Alessandra Micheletti, Junichi Nakagawa, Alessio A. Alessi, Vincenzo Capasso, Davide Grimaldi, Daniela Morale, and Elena Villa

Abstract Dual Phase steel (DP steel) has shown high potential for automotive and other applications, due to its remarkable combined properties of high strength and good formability. The mechanical properties of the material are strictly related to the spatial distribution of the two steel phases, ferrite and martensite, and with their stochastic geometry. Unfortunately the experimental costs to obtain images of sections of steel samples are very high, so that one important industrial problem is to reduce the required number of 2D sections in order to either reconstruct the 3D geometry of the material, or to simulate realistic ones. In this work we will present a germ-grain statistical model which can be used for a best fitting of the main geometric characteristics of the martensite phase. The parameters of the model are estimated on the basis of morphological characteristics of the images of about 150 tomographic sections taken from a real sample. After optimization or tuning of the relevant parameters, the statistical model can then be used to identify the minimum number of sections of the sample which are needed to estimate the parameters in a reliable way.

Keywords Dual phase steel • Germ-grain model • Mathematical morphology

A. Micheletti (✉)
Department of Mathematics and ADAMSS Center, Università degli Studi di Milano, Milano, Italy
e-mail: alessandra.micheletti@unimi.it

J. Nakagawa
Mathematical Science & Technology Research Lab, Nippon Steel & Sumitomo Metal, Tokyo, Japan

A.A. Alessi • D. Grimaldi • D. Morale • E. Villa
Department of Mathematics, Università degli Studi di Milano, Milano, Italy

V. Capasso
Gregorio Millan Institute, Escuela Politecnica Superior, Universidad Carlos III de Madrid, Leganes, Spain

ADAMSS Center, Università degli Studi di Milano, Milano, Italy

G. Russo et al. (eds.), *Progress in Industrial Mathematics at ECMI 2014*,
Mathematics in Industry 22, DOI 10.1007/978-3-319-23413-7_105

1 Introduction

Dual Phase steels (DP steels) have shown high potential for many applications due to their remarkable property combination between high strength and good formability.

Here we consider a sample of steel formed by martensite and ferrite. The relative position and geometric structure of the two phases is responsible of the mechanical properties of the material, thus it is particularly important to provide statistical models which may reproduce the main geometric characteristics of the two phases. Our results are based on images of about 150 tomographic sections taken from a lab sample of steel.

The formation of the two phases of the material starts after a cooling phase of the melted alloy of iron and carbon, during which austenite is formed, followed by a rolling phase, transforming slabs of steel into thin metal foils.

A further cooling phase follows the rolling; during this phase the formation of ferrite starts. Crystals of ferrite nucleate mainly from the interfaces of the rolled (and thus deformed) austenite, and grow up to impingement with other crystals of ferrite, driven by the evolving field of carbon concentration. After a fixed time interval the formation of ferrite is stopped by a sudden quenching, during which the material still not transformed into ferrite becomes martensite. The final result is a dual phase steel formed by ferrite and martensite, having a stochastic geometric structure.

In order to define a dynamical model able to reproduce the complete geometric structure of the material, a stochastic birth and growth process coupled with the evolution of the carbon field should be used (see [1] for a similar model applied to polymer crystallization). A first model which goes in this direction, though facing the problem at only a macroscopic scale, has been studied in [4].

In the following we will introduce a germ-grain model which may reproduce the main mean geometric characteristics of the martensite contained in the real sample.

As from a confidentiality agreement with Nippon Steel & Sumitomo Metal, who provided the real data, the images of the real sample will not be shown.

2 Structure of the Austenite Phase

First of all we studied the geometric structure of the interfaces of austenite after rolling, since nucleation of ferrite happens mainly on such interfaces, so that the location of the final ferrite and martensite crystals depends on the location of such interfaces.

The shape of the crystals of austenite before rolling is quite close to a 3D Voronoi tessellation. The rolling reduces the thickness of the rolled slab to 1/50 of the original thickness, but preserving the width and the total volume. The result is a long thin foil (see Fig. 1).

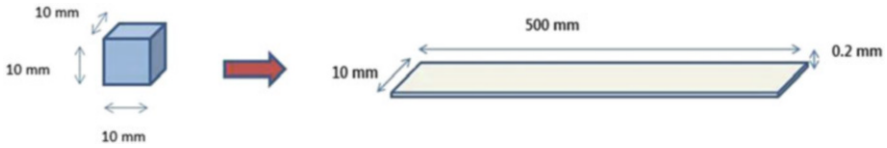

Fig. 1 Deformation applied to the cube containing the 3D Voronoi tessellation formed by austenite crystals

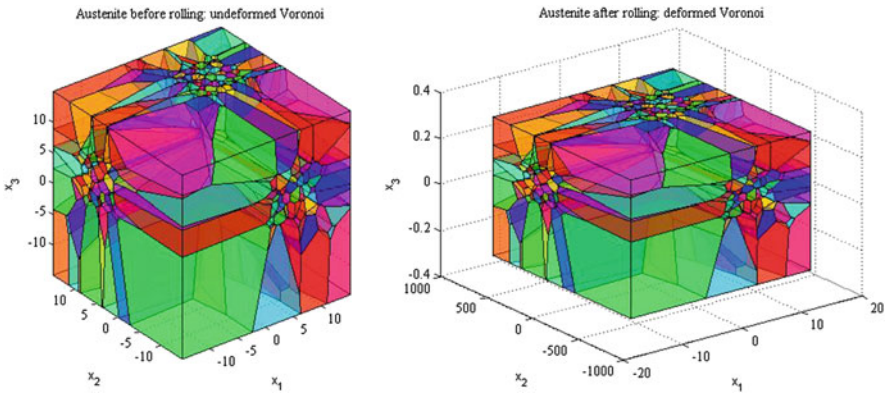

Fig. 2 Voronoi tessellation of the 3D space with 3000 crystals in a cube. On the *left*: before rolling, on the *right*: after rolling. The different axes scales in the two images evidentiate the deformation along the three axes, due to rolling

If we apply a deformation to a 3D Voronoi tessellation, maintaining the proportions used in the real experimental situation, we obtain the results shown in Fig. 2.

Since the real sample is composed by a very small portion of the rolled metal foil, extracted from the middle of the foil, we sectioned a small cube of the deformed tessellation, with dimensions proportional to the real sample, to look at its internal geometric structure. Two sections in the x_1x_3 and x_2x_3 direction, respectively, are reported in Fig. 3.

It is evident that, at the scales relevant for our application, the effect of rolling is to transform the interfaces of the 3D Voronoi tessellation into approximately parallel planes, having random quotes along the x_3 axis. The distribution of the quotes looks quite regular. This is in accordance with the images of sections of austenite after rolling, which shows a typical pancake structure (see Fig. 4).

We thus modelled the interfaces of austenite as parallel horizontal planes, i.e. parallel to direction x_1x_2, with randomly distributed quotes along the x_3 axis. The quotes have been distributed according to a 1-dimensional hard core process [3, Sect. 5.4], that is a point process with an inhibition distance between points. Figure 4 on the right shows a simulated realization of such a process.

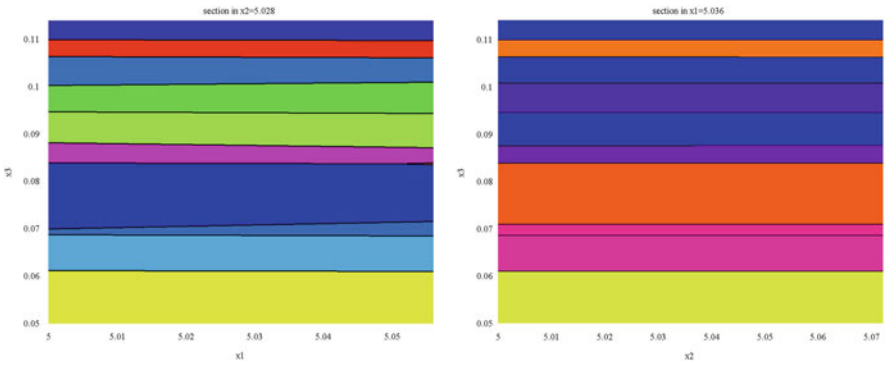

Fig. 3 Two sections of the deformed Voronoi tesselation on the *right* of Fig. 2, taken in the center of the parallelepiped. On the *left*: section parallel to the x_1x_3 plane; on the *right*: section parallel to the x_2x_3 plane. *Different colours* correspond to different crystals

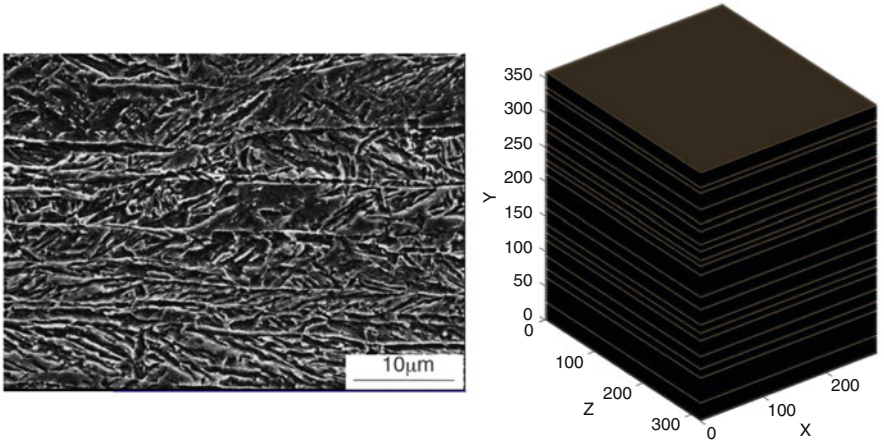

Fig. 4 On the *left*: pancake structure of austenite after rolling and before the birth and growth of ferrite; on the *right*: simulated random parallel planes, with an inhibition distance, from which the nucleation of ferrite starts

In Fig. 5 a simulated sample of the two phases which resembles the real one is reported. The black region, occupied by martensite, can be represented as the free space between different crystals of ferrite at the moment of quenching. Since the crystals of ferrite nucleate on the parallel planes representing the interfaces of austenite, martensite will have a tendency to concentrate in between two adjacent parallel planes.

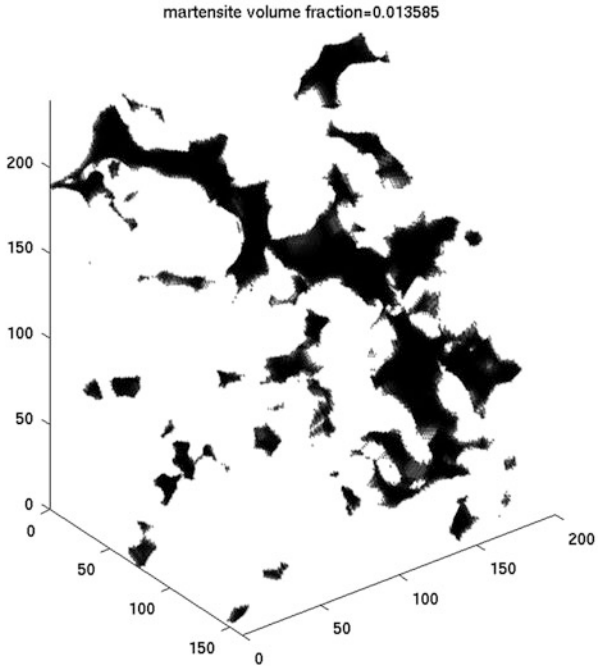

Fig. 5 A simulated sample of the two phases: the region occupied by martensite is depicted in *black*, while ferrite is in *white*

3 A Germ-Grain Model

In order to set up a statistical model able to reproduce the mean geometric structure of martensite, we have defined a germ-grain model with spherical grains, depending on a small set of unknown parameters.

A germ-grain model is a random closed set $\Xi \subseteq \mathbb{R}^d$ defined as

$$\Xi = \cup_{i \in \mathbb{N}} \Theta_i \oplus x_i$$

where $\{x_i\}$ are points in $\mathbb{R}^d$ forming a locally finite point process, called *germs*; Θ_i are i.i.d. uniformly bounded random closed sets (usually containing the origin) called *grains*, and $\oplus$ denotes the Minkowski sum between sets, thus $\Theta_i \oplus x_i = \{y + x_i | y \in \Theta_i\}$ (for more details see [2, 3]).

We modelled the point process of germs as a Neyman-Scott clustered point process, taking into account that martensite is formed in between the nucleation planes of ferrite, and also observing that martensite in the real sample exhibits a cluster structure.

The Neyman-Scott point process [3, Sect. 5.3] is formed by generating a spatial Poisson point process of *parents* having intensity $\lambda_p(x)$ and then surrounding

the parents by a random number of *daughter points*, scattered independently and identically distributed around the parents. The parents are then removed and the Neyman-Scott process is formed just by the daughter points.

The germs in our model have thus been generated according to the following algorithm:

Algorithm 1

Input:
n_{planes} = Number of parallel planes,
σ_{vert}= standard deviation of the daughters' distribution in vertical direction,
σ_{hor}=standard deviation of the daughters' distribution in horizontal direction,

1. randomly generate a set of parallel planes, as in Fig. 4, from which ferrite nucleates;
2. build up a set of "virtual" parallel planes, from which martensite originates, each located in the middle of two adjacent planes of the previous set;
3. distribute the parent germs uniformly on the "virtual" parallel planes;
4. distribute the daughter germs around the parents according to a 3-variate normal distribution having diagonal covariance matrix given by

$$\Sigma = diag(\sigma_{hor}^2, \sigma_{hor}^2, \sigma_{vert}^2).$$

The grains have been modeled as independent spheres of random radius $R = L{\cdot}\rho$, where L is a constant representing the maximum possible radius of the spheres and ρ is a random variable distributed as a $Beta(2, b)$ with $b > 2$. The reason of this choice is that in this way smaller spheres are privileged, providing to the germ grain model an aspect closer to the real sample.

The number of germs in the model is random, and has been generated according to the following procedure. Since the volume fraction occupied by martensite in the real sample is 0.027, we generated iteratively new germs and grains up to when the volume fraction occupied by the germ-grain model overcame 0.027. We made this choice since usually the percentage of martensite contained in steel is a known parameter, which can be measured even without sectioning the material.

In order to avoid edge effects, the simulation of the model has been performed in a window of observation enlarged by L on each side, and then only the central portion of the window with dimensions equal to the real sample has been considered. All the simulations have been performed in Matlab.

Thus our germ grain model is based on the following five parameters:

$$(n_{planes}, \sigma_{hor}, \sigma_{vert}, L, b) \in \mathbb{N} \times \mathbb{R}_+ \times \mathbb{R}_+ \times \mathbb{N} \times [2, +\infty) \tag{1}$$

4 Parameters Estimate

In order to estimate the parameters of the model we considered the 2D images of the about 150 sections of the real sample and for each section we computed the following geometric characteristics:

1. A = the area of the region occupied by martensite, measured in pixels;
2. P = the perimeter of the region occupied by martensite, computed by calculating the distance between each adjoining pair of pixels around the border of the region;
3. A_{hull} = area of the convex hull of martensite;
4. D = diameter of a circle with the same area of martensite;
5. E = Euler number i.e. the number of connected components of martensite in the region minus the number of holes in the components;
6. O = orientation, i.e. the angle between the x-axis and the major axis of the ellipse that has the same second-moments as the region occupied by martensite;
7. M = length (in pixels) of the major axis of the ellipse that has the same normalized second central moments as the region occupied by martensite;
8. m = length (in pixels) of the minor axis of the ellipse that has the same normalized second central moments as the region occupied by martensite.

For each set of the parameters (1) we performed 30 simulations of the germ grain model, and we sectioned the simulated images into the same number of parts of the real sample. On each simulated section we computed the eight geometric characteristics listed above.

The parameters can be estimated by minimizing a suitable distance between the values of the geometric characteristics measured on the real sample and the mean geometric characteristics of the simulated germ-grain model. Since we measured 8 variables for each section, resulting in a huge number of variables, we reduced the dimension of the problem by applying a principal component analysis to the $8 \times (n.\ of\ sections)$ variables, retaining only the first three principal components, which explain about the 40 % of the total variance of the simulations.

Let us denote by $\underline{G}_{real} \subseteq \mathbb{R}^3$, the first three PC's computed on the real sample, by $\bar{\underline{G}}_{sim}(\underline{p}) \subseteq \mathbb{R}^3$ the means, over 30 simulations, of the first three PC's computed on the simulated samples, and by S the sample covariance matrix of the first three PC's computed on the simulations.

For minimizing with respect to the parameters $\underline{p} = (n_{planes}, \sigma_{hor}, \sigma_{vert}, L, b)$, we have adopted the Mahalanobis distance

$$\Delta(\underline{G}_{real}, \bar{\underline{G}}_{sim}(\underline{p})) = \sqrt{(\underline{G}_{real} - \bar{\underline{G}}_{sim}(\underline{p}))^T S^{-1} (\underline{G}_{real} - \bar{\underline{G}}_{sim}(\underline{p}))}, \tag{2}$$

Table 1 Optimal values of the parameters. The corresponding computed Mahalanobis distance is 0.09. The simulations have been performed in a parallelepiped formed by $160 \times 200 \times 240$ voxels, where the side of each voxels is $0.25\,\mu$m long. The unit of measure of the parameters is a voxel side length

Parameter	Optimal value
n_{planes}	32
σ_{hor}	14.69
σ_{vert}	70.33
L	9
b	3.8

since it weights the distance from the mean of the simulations with the variance, taking thus into account the variability related with each set of parameters. Note that the distance (2) is stochastic, being based on the outcomes of random simulations.

Since both parameters n_{planes} and L are integers (the maximum side of the spheres has been defined in the simulation program in terms of number of voxels), we needed to apply an optimization algorithm to a function which is not expressed in algebraic form and depending upon mixed integer and real parameters, so that we have decided to apply a genetic algorithm for the best fitting

$$\underline{\hat{p}} = \arg\min_{\underline{p}} \Delta(\underline{G}_{real}, \bar{\underline{G}}_{sim}(\underline{p})).$$

The estimated parameters are reported in Table 1.

In Fig. 6 the following results obtained by simulating the germ grain model are reported: the top figure represents a "cloud" of 50 points with coordinates equal to the first three principal components of $\underline{G}_{sim}$, each computed on a different simulation performed with the optimal parameters. The black bold dot represents the first three principal components of $\underline{G}_{real}$, it is almost in the center of the cloud and very close to the mean of the principal components of the simulated patterns, showing thus a good agreement between the fitted model and the real data. The two bottom figures visualize the results of one single simulation of the germ grain model performed with the optimal parameters, and a section of the simulated pattern in direction orthogonal to the Z axis. These images must be compared with the corresponding ones of the real sample. At a first visual inspection, we may observe a rather good agreement between the simulation and the real sample, thus confirming the effectiveness of the adopted method.

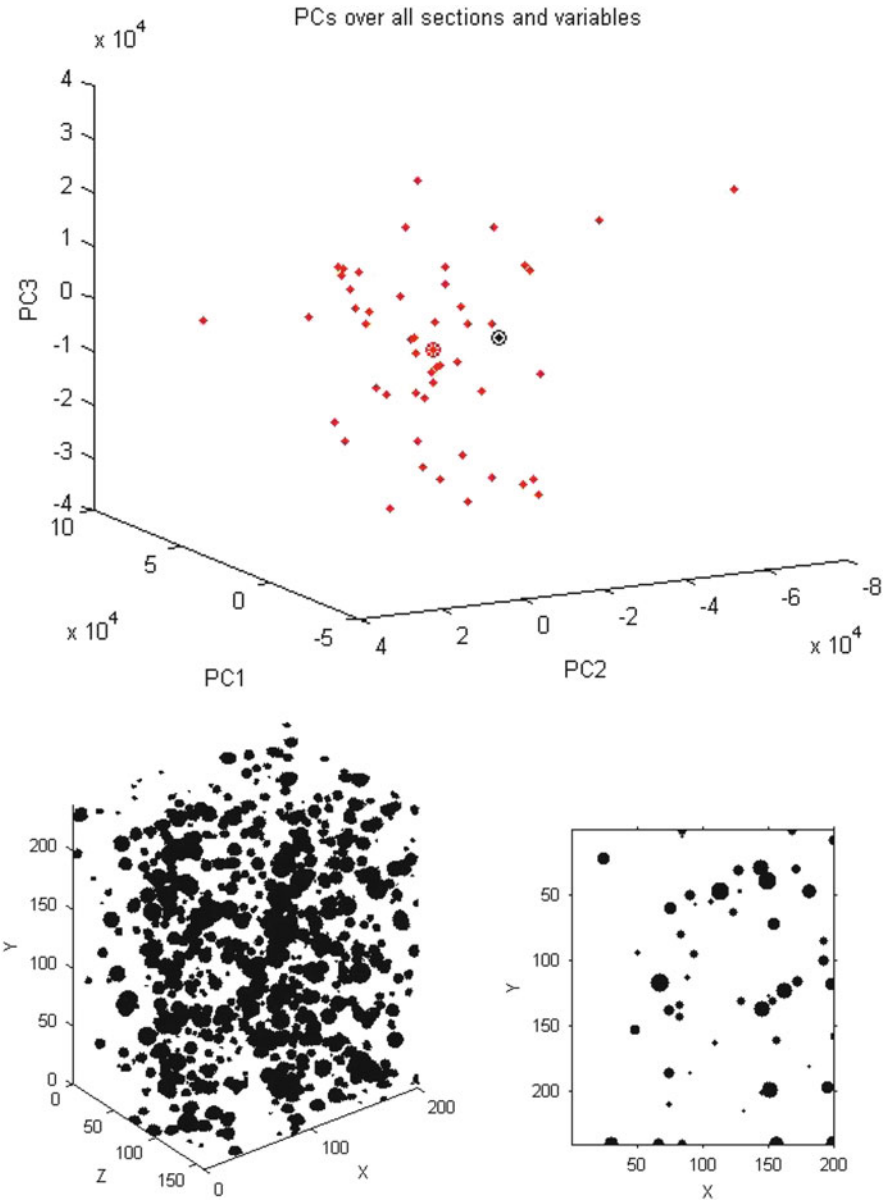

Fig. 6 *Top figure*: the first three PC's of 50 simulations performed with the optimal parameters (*red dots*), their mean (*red bold dot*), and the first three PC's of the real sample (*black bold dot*); *bottom left*: a simulation of the germ grain model with the optimal parameters; *bottom right*: a section orthogonal to Z direction of the simulation

References

1. Capasso, V. (ed.): Mathematical Modelling for Polymer Processing. Polymerization, Crystallization, Manufacturing. Mathematics in Industry, vol. 2. Springer, Heidelberg (2003)
2. Matheron, G.: Random Sets and Integral Geometry. Wiley, New York (1975)
3. Stoyan, D., Kendall, W.S., Mecke, J.: Stochastic Geometry and Its Application. Wiley, New York (1995)
4. Suwanpinij, P., Togobytska, N., Prahl, U., Weiss, W., Hömberg, D., Bleck, W.: Numerical cooling strategy design for hot rolled dual phase steel. Steel Res. Int. **81**, 1001–1009 (2010)